INTERNATIONAL JOURNAL FOR NUMERICAL METHODS IN ENGINEERING
Int. J. Numer. Meth. Engng 2007; **69**:1570–1589
Published online 31 July 2006 in Wiley InterScience (www.interscience.wiley.com). DOI: 10.1002/nme.1826

The method of fundamental solutions for inverse source problems associated with the steady-state heat conduction

Bangti Jin[1,*,†] and Liviu Marin[2]

[1]*Department of Mathematics, The Chinese University of Hong Kong, Shatin, New Territory, Hong Kong SAR, People's Republic of China*
[2]*School of Mechanical, Materials and Manufacturing Engineering, The University of Nottingham, University Park, Nottingham NG7 2RD, U.K.*

SUMMARY

This paper presents the use of the method of fundamental solutions (MFS) for recovering the heat source in steady-state heat conduction problems from boundary temperature and heat flux measurements. It is well known that boundary data alone do not determine uniquely a general heat source and hence some *a priori* knowledge is assumed in order to guarantee the uniqueness of the solution. In the present study, the heat source is assumed to satisfy a second-order partial differential equation on a physical basis, thereby transforming the problem into a fourth-order partial differential equation, which can be conveniently solved using the MFS. Since the matrix arising from the MFS discretization is severely ill-conditioned, a regularized solution is obtained by employing the truncated singular value decomposition, whilst the optimal regularization parameter is determined by the L-curve criterion. Numerical results are presented for several two-dimensional problems with both exact and noisy data. The sensitivity analysis with respect to two solution parameters, i.e. the number of source points and the distance between the fictitious and physical boundaries, and one problem parameter, i.e. the measure of the accessible part of the boundary, is also performed. The stability of the scheme with respect to the amount of noise added into the data is analysed. The numerical results obtained show that the proposed numerical algorithm is accurate, convergent, stable and computationally efficient for solving inverse source problems in steady-state heat conduction. Copyright © 2006 John Wiley & Sons, Ltd.

Received 18 February 2006; Revised 23 May 2006; Accepted 5 June 2006

KEY WORDS: method of fundamental solutions; inverse source problem; truncated singular value decomposition; steady-state heat conduction

*Correspondence to: Bangti Jin, Department of Mathematics, The Chinese University of Hong Kong, Shatin, New Territory, Hong Kong SAR, People's Republic of China.
†E-mail: kimbtsing@yahoo.com.cn

1. INTRODUCTION

Inverse source problems arise in many branches of science and engineering, e.g. heat conduction, crack identification, electromagnetic theory, geophysical prospecting and pollutant detection. In heat conduction, the interior heat source is sought from the measurements of the temperature and heat flux on the boundary. It is well known that a general source is not determined uniquely by the boundary measurements. For a complete discussion of the theoretical aspects of this problem, we refer the reader to the monograph [1]. The inverse source problem becomes solvable if some *a priori* knowledge is assumed. For instance, if one of the products in the separation of variables is known [2], the base area of a cylindrical source is known [2], the sought source is a characteristic function [1] or a point source [3], then the boundary data can uniquely determine the unknown source. In the present study, the source is assumed to satisfy a second-order partial differential equation on a physical basis.

Reconstructing point sources has received much attention and several efficient numerical algorithms, such as algebraic reconstruction and projection method, have been proposed. For an overview of the state of the art, we refer the reader to References [3, 4], as well as the references therein. The recovery of a general source presents difficulty and only a limited number of papers devoted to this subject are available in the literature. The reconstruction of a general source has been previously considered by Kagawa *et al.* [5, 6] and Trlep *et al.* [7], who employed the dual reciprocity method (DRM) to approximate $f(\mathbf{x})$ and the boundary element method (BEM) to discretize the governing equation. However, they have only tested the proposed methods on several examples using exact data and failed to note the non-uniqueness of the solution. Matsumoto *et al.* [8, 9] also applied the DRM and BEM to the numerical solution for examples with exact data only. Farcas *et al.* [10] investigated numerically the non-uniqueness of the problem and they proposed the Tikhonov regularization method, in conjunction with the DRM, for recovering the minimum-norm solution, which usually is the solution of the most practical interest and relevance from the many solutions of the source reconstruction problem. However, it was not shown that the regularized solution is guaranteed to be of minimum-norm since the Tikhonov regularization method imposes the minimum-norm constraint on the coefficient vector used in the DRM, which is only indirectly related to the minimum-norm heat source. El Badia *et al.* [11] applied an iterative method, namely the Hilbert uniqueness method, to recover the harmonic component of the general source, while the finite element method (FEM) was employed to discretize the Poisson equation.

The BEM reduces the dimensionality of the problem by one and thus it is useful for solving linear problems. However, it requires the evaluation of singular integrals, suffers from slow convergence due to the use of lower-order polynomials and requires the meshing of the boundary, which can be difficult for complicated geometries in high dimensions. The method of fundamental solutions (MFS) [12–14] avoids the difficulties associated with the BEM. It is a boundary-type meshfree technique for the solution of partial differential equations and it has become very popular in recent years due to its ease of implementation. In the present paper, we investigate a numerical scheme based on the MFS, in conjunction with the truncated singular value decomposition (TSVD), for solving the inverse source problem associated with the steady-state heat conduction. It should be noted that the MFS, in conjunction with regularization methods, has recently been applied to inverse problems with great success, such as the Cauchy problem for various partial differential equations [15–20] and inverse heat conduction problems [21, 22].

The paper is organized as follows: In Section 2, we formulate the problem mathematically. Section 3 is devoted to the numerical algorithm: The MFS used for discretizing the partial differential

DOI: 10.1002/nme

equation and the TSVD employed for solving ill-conditioning matrix equations are described. In Section 4, we present numerical results for several two-dimensional problems with both exact and noisy data. Finally, concluding remarks are given in Section 5.

2. MATHEMATICAL FORMULATION OF THE PROBLEM

Let Ω be an open bounded domain in $\mathbb{R}^d$, where d is the dimensionality of the space and $\Gamma = \partial\Omega$ is its boundary. The steady-state heat conduction in an isotropic medium is described by the Poisson equation, namely

$$\mathscr{L}u(\mathbf{x}) = \sum_{i=1}^{d} \frac{\partial^2 u(\mathbf{x})}{\partial x_i^2} = f(\mathbf{x}), \quad \mathbf{x} = (x_1, \ldots, x_d) \in \Omega \tag{1}$$

The heat flux $q(\mathbf{x})$ through the boundary Γ is given by

$$q(\mathbf{x}) = \frac{\partial u}{\partial n}, \quad \mathbf{x} \in \Gamma \tag{2}$$

where $n(\mathbf{x})$ is the outward unit vector normal to the boundary Γ.

Assume that the source term $f(\mathbf{x})$ is unknown and both the temperature and heat flux can be measured on an accessible part of the boundary $\Gamma_1 \subset \Gamma$, i.e.

$$u(\mathbf{x}) = g(\mathbf{x}), \quad q(\mathbf{x}) = h(\mathbf{x}), \quad \mathbf{x} \in \Gamma_1 \tag{3}$$

It should be mentioned that data may be available at a few measurement points only. This problem is mathematically under-determined and hence some additional *a priori* assumptions on the source should be made in order to guarantee the uniqueness of the solution.

In several practical applications, such as magnetoencephalography (MEG) and electroencephalography (EEG), the source is assumed to be a point source. However, point sources cannot generate an effect equivalent to that of body sources [23] and practically all sources are of body-type. Therefore, it would be interesting to perform the reconstruction of body sources. However, the inverse problem of recovering a general source does not admit a unique solution. A minimum-norm solution to this problem is usually that of practical interest according to the so-called 'principle of parsimony' [24], which states that, from the multitude of solutions to the inverse problem, the one that reveals the least amount of details or information should be selected. This has been previously exploited by Farcas *et al.* [10] to explain their results obtained using the Tikhonov regularization method. It turns out that the minimum-norm solution should satisfy the Laplace equation [2], which gives rise to the following formulation of the problem:

Formulation 1. The source satisfies the homogeneous Laplace equation $\mathscr{L}f(\mathbf{x}) = 0$, i.e. the source is harmonic in Ω. Applying the operator $\mathscr{L}$ to both sides of Equation (1) gives

$$\begin{aligned} \mathscr{L}^2 u(\mathbf{x}) &= 0, \quad \mathbf{x} \in \Omega \\ u(\mathbf{x}) &= g(\mathbf{x}), \quad \mathbf{x} \in \Gamma_1 \\ q(\mathbf{x}) &= h(\mathbf{x}), \quad \mathbf{x} \in \Gamma_1 \end{aligned} \tag{4}$$

DOI: 10.1002/nme

In order to illustrate the facility of the proposed scheme for incorporating other *a priori* assumptions involving a differential operator, we also consider the following:

Formulation 2. The source satisfies the homogeneous modified Helmholtz equation $(\mathscr{L} - \lambda^2) f(\mathbf{x}) = 0$, with the wave number λ known. The *a priori* assumption corresponds to the minimum-norm solution in the case of heat conduction in a fin, which could be described by the modified Helmholtz equation [25]. However, its engineering implication is not clear in the current context. Applying the operator $\mathscr{L} - \lambda^2$ to both sides of Equation (1) gives

$$\begin{aligned} (\mathscr{L} - \lambda^2)\mathscr{L} u(\mathbf{x}) &= 0, \quad \mathbf{x} \in \Omega \\ u(\mathbf{x}) &= g(\mathbf{x}), \quad \mathbf{x} \in \Gamma_1 \\ q(\mathbf{x}) &= h(\mathbf{x}), \quad \mathbf{x} \in \Gamma_1 \end{aligned} \tag{5}$$

Although other formulations of the problem may be possible, in this study we investigate only the aforementioned two formulations of the inverse source problem. It should be noted that our *a priori* assumption rules out the case of point sources, which are of interest in several important applications. Adapting the MFS for the reconstruction of point sources will be considered separately.

3. NUMERICAL ALGORITHM

In this section, we describe the numerical scheme for solving the inverse source problem, namely the MFS, in conjunction with the TSVD. Rules for choosing an appropriate regularization parameter are also detailed.

3.1. The method of fundamental solutions

The MFS was originally introduced by Kupradze and Aleksidze [26] and later numerically implemented by Mathon and Johnston [27]. The basic idea of the method is to approximate the solution of the governing partial differential equation by a linear combination of fundamental solutions with singularities, also known as source points, located on a fictitious boundary outside the solution domain. For detailed theoretical grounds of the method and its wide range of application to forward problems, we refer the reader to the comprehensive surveys [12–14, 28] and the references therein. The MFS has recently been applied to inverse problems, such as the Cauchy problem for Helmholtz-type equations [15–17] and the Navier system in linear elasticity [19, 20], and inverse heat conduction problems [18, 21, 22]. Motivated by the encouraging results reported in these works, we aim to adapt the MFS for inverse source problem in the current investigation.

The fundamental solution for the Laplace operator $\mathscr{L}$ is given by [29]

$$u^*_{\mathscr{L}}(\mathbf{x}) = \begin{cases} -\dfrac{1}{2\pi} \ln r, & \mathbf{x} \in \mathbb{R}^2 \\ \dfrac{1}{4\pi r}, & \mathbf{x} \in \mathbb{R}^3 \end{cases} \tag{6}$$

where $r = \|\mathbf{x}\|_2$ and $\|\cdot\|_2$ denotes the Euclidean norm.

DOI: 10.1002/nme

The fundamental solution to the biharmonic operator $\mathscr{L}^2$ is given by

$$u^*_{\mathscr{L}^2}(\mathbf{x}) = \begin{cases} -\dfrac{1}{2\pi} r^2 \ln r, & \mathbf{x} \in \mathbb{R}^2 \\ \dfrac{r}{4\pi}, & \mathbf{x} \in \mathbb{R}^3 \end{cases} \tag{7}$$

The fundamental solution for the modified Helmholtz operator $\mathscr{L} - \lambda^2$ is given by

$$u^*_{\mathscr{L}-\lambda^2}(\mathbf{x}) = \begin{cases} \dfrac{1}{2\pi} K_0(\lambda r), & \mathbf{x} \in \mathbb{R}^2 \\ \dfrac{1}{4\pi r} e^{-\lambda r}, & \mathbf{x} \in \mathbb{R}^3 \end{cases} \tag{8}$$

where K_0 is the modified Bessel functions of the second kind of order zero.

In the MFS, the solution of the partial differential equation is approximated by a linear combination of the fundamental solutions [30, 31], namely

$$u(\mathbf{x}) = \sum_{j=1}^{n_s} a_j G_j(\mathbf{x}) + \sum_{j=1}^{n_s} b_j H_j(\mathbf{x}) \quad \text{for } \mathbf{x} \in \Omega \tag{9}$$

where n_s is the number of source points and $\{a_j, b_j\}$ are unknown coefficients to be determined. The basis functions $G_j(\mathbf{x})$ and $H_j(\mathbf{x})$ are defined as follows:

$$G_j(\mathbf{x}) = u^*_{\mathscr{L}}(\mathbf{x} - \mathbf{y}_j) \tag{10}$$

and

$$H_j(\mathbf{x}) = \begin{cases} u^*_{\mathscr{L}^2}(\mathbf{x} - \mathbf{y}_j), & \text{Formulation 1} \\ u^*_{\mathscr{L}-\lambda^2}(\mathbf{x} - \mathbf{y}_j), & \text{Formulation 2} \end{cases} \tag{11}$$

respectively, where $\{\mathbf{y}_j\}$ are source points located on a fictitious boundary outside the solution domain.

Although the approximate solution $u(\mathbf{x})$ automatically satisfies the partial differential equation (4) or (5), it does not necessarily satisfy the associated boundary conditions. The latter can be achieved by the means of the collocation method. Let $\{\mathbf{x}_i\}$ be a set of points chosen on the accessible part of the boundary Γ_1. By collocating the boundary conditions at $\{\mathbf{x}_i\}$, we arrive at the following system of algebraic equations:

$$\begin{aligned} g(\mathbf{x}_i) &= \sum_{j=1}^{n_s} a_j G_j(\mathbf{x}_i) + \sum_{j=1}^{n_s} b_j H_j(\mathbf{x}_i), \quad i = 1, 2, \ldots, n_b \\ h(\mathbf{x}_i) &= \sum_{j=1}^{n_s} a_j \partial_n G_j(\mathbf{x}_i) + \sum_{j=1}^{n_s} b_j \partial_n H_j(\mathbf{x}_i), \quad i = 1, 2, \ldots, n_b \end{aligned} \tag{12}$$

where n_b is the number of collocation points on the accessible part of the boundary Γ_1 and ∂_n denotes taking the normal derivative.

DOI: 10.1002/nme

Briefly, the following matrix equation is obtained:

$$\mathbf{A}\mathbf{a} = \mathbf{b} \tag{13}$$

where $\mathbf{a} = (a_1, a_2, \ldots, a_{n_s}, b_1, b_2, \ldots, b_{n_s})^{\mathrm{T}}$ is the unknown coefficient vector and $\mathbf{b}$ is the data vector. The matrix $\mathbf{A} = (A_{ij})$ is an interpolation matrix with the entries A_{ij} defined by

$$A_{ij} = \begin{cases} G_j(\mathbf{x}_i), & i = 1, 2, \ldots, n_b, \quad j = 1, 2, \ldots, n_s \\ H_{j-n_s}(\mathbf{x}_i), & i = 1, \ldots, n_b, \quad j = n_s + 1, \ldots, 2n_s \\ \partial_n G_j(\mathbf{x}_{i-n_b}), & i = n_b + 1, \ldots, 2n_b, \quad j = 1, 2, \ldots, n_s \\ \partial_n H_{j-n_s}(\mathbf{x}_{i-n_b}), & i = n_b + 1, \ldots, 2n_b, \quad j = n_s + 1, \ldots, 2n_s \end{cases} \tag{14}$$

In order to implement the MFS, the location of the source points has to be determined and this is usually achieved by considering either the static or the dynamic approach. In the static approach, the source points are pre-assigned and kept fixed throughout the solution process, whilst in the dynamic approach, the source points and the unknown coefficients are determined simultaneously during the solution process [13]. Moreover, Mitic and Rashed [32] have shown that the distribution of the source points is not important under minor conditions. Therefore, we have decided to employ the static approach in our computations.

3.2. Truncated singular value decomposition

The MFS can be regarded as a Fredholm integral equation of the first kind with an analytical kernel function, which is severely ill-posed according to the theory of integral equations. Consequently, as an approximation to the integral operator, the interpolation matrix $\mathbf{A}$ is severely ill-conditioned. The accurate and stable solution of Equation (13) is very important for obtaining physically meaningful numerical results. Regularization methods [33] are among the most popular and successful methods for solving stably and accurately ill-conditioned matrix equations. In our computations we use the TSVD to solve the matrix equation arising from the MFS discretization.

The singular value decomposition (SVD) of a matrix $\mathbf{A} \in \mathbf{R}^{m \times n} (m \geqslant n)$ is given by

$$\mathbf{A} = \mathbf{U}\mathbf{\Sigma}\mathbf{V}^{\mathrm{T}} \tag{15}$$

where $\mathbf{U} = [\mathbf{u}_1, \mathbf{u}_2, \ldots, \mathbf{u}_m]$ and $\mathbf{V} = [\mathbf{v}_1, \mathbf{v}_2, \ldots, \mathbf{v}_n]$ are orthonormal matrices with column vectors called the left and the right singular vectors, respectively, T denotes the matrix transposition and $\mathbf{\Sigma} = \mathrm{diag}(\sigma_1, \sigma_2, \ldots, \sigma_n)$ is a diagonal matrix with non-negative diagonal elements in non-increasing order, which are the singular values of $\mathbf{A}$.

On using the SVD, the solution $\mathbf{a}$ to the matrix equation (13) can be succinctly written as a linear combination of the right singular vectors, namely

$$\mathbf{a} = \sum_{i=1}^{k} \frac{\mathbf{u}_i^{\mathrm{T}}\mathbf{b}}{\sigma_i}\mathbf{v}_i \tag{16}$$

where k is the rank of the matrix $\mathbf{A}$. For an ill-conditioned matrix equation, there are many small singular values clustering around zero and therefore the solution obtained by standard methods, such as the Gauss elimination method, may be dominated by the contribution of the small

DOI: 10.1002/nme

singular values and hence it becomes unbounded and oscillatory. One simple remedy is to truncate the above summation, i.e. by considering an approximate solution, $\mathbf{a}^p$, given by

$$\mathbf{a}^p = \sum_{i=1}^{p} \frac{\mathbf{u}_i^{\mathrm{T}}\mathbf{b}}{\sigma_i}\mathbf{v}_i \tag{17}$$

where $p \leqslant k$ is the regularization parameter which determines when one starts to leave out small singular values. This method is known as the TSVD [33] in the inverse problem community and the principal component analysis (PCA) in statistics.

The performance of regularization methods depends crucially on the suitable choice of the regularization parameter. One extensively studied criterion is the discrepancy principle [33]. Although this criterion is mathematically rigorous, it requires a reliable estimation of the amount of noise added into the data which may not be available in practical problems. Heuristical approaches are more preferable in the case when no *a priori* information about the noise is available. For the TSVD, several heuristical approaches have been proposed, including the L-curve criterion and the generalized cross-validation. In this paper, we employ the L-curve criterion [34] to determine an appropriate regularization parameter for the TSVD.

If we define the following curve:

$$L = \{(\log(\|\mathbf{a}^i\|_2), \log(\|\mathbf{A}\mathbf{a}^i - \mathbf{b}\|_2)),\ \ i = 1, 2, \ldots, k\} \tag{18}$$

then this typically has an L-shaped form and hence it is known as the L-curve. According to the L-curve criterion, the optimal regularization parameter corresponds to the corner of the L-curve since a good tradeoff between the residual and solution norms is achieved at this point. Numerically, the L-curve method is robust and stable with respect to both uncorrelated and highly correlated noise. Furthermore, this criterion works effectively with certain classes of practical problems [33–35] and, for a discussion of the theoretical aspect of the L-curve criterion, we refer the reader to References [36, 37]. Several algorithms for locating the corner of the L-curve have been reported in the literature, see e.g. References [33, 38–40]. The first procedure [33] is based on fitting a parametric cubic spline to the discrete points and then taking the point corresponding to the maximum curvature of the L-curve to be its corner. The second algorithm employs a conic to fit the set of discrete points [38], whilst the third one is based on using a linear-linear scale and inverting the axis [39]. All these procedures need to check the monotonicity condition for the sequences of the residual and solution norms, and discard those points where the monotonicity condition is not fulfilled. The last algorithm, namely the triangle method, is based on geometric considerations, see e.g. Reference [40]. In the present study, we mainly employ the first algorithm. However, the curvature of the parametric spline is very sensitive to the node distribution and occasionally the located corner is not suitable [34]. Therefore, visual inspection is used as an auxiliary procedure.

Once the coefficients $\{a_j, b_j\}$ are determined, the numerical solution for the heat source can be easily obtained by applying the Laplace operator $\mathscr{L}$ to the approximate solution $u(\mathbf{x})$. To be more precise, the approximate solution $f(\mathbf{x})$ to the heat source is given by

$$f(\mathbf{x}) = \sum_{j=1}^{n_s} a_j \mathscr{L} G_j(\mathbf{x}) + \sum_{j=1}^{n_s} b_j \mathscr{L} H_j(\mathbf{x}) \tag{19}$$

DOI: 10.1002/nme

where the first term on the right-hand side vanishes due to the harmonicity of the basis function $G_j(\mathbf{x})$. For Formulation 1 in the two-dimensional case, we have

$$\mathscr{L}H_j(\mathbf{x}) = \left(\frac{\partial^2}{\partial x_1^2} + \frac{\partial^2}{\partial x_2^2}\right)\left(-\frac{1}{2\pi}\|\mathbf{x}-\mathbf{y}_j\|^2 \ln\|\mathbf{x}-\mathbf{y}_j\|\right) \tag{20}$$

$$= -\frac{1}{2\pi}(4\ln\|\mathbf{x}-\mathbf{y}_j\| + 4) = 4\left(G_j(\mathbf{x}) - \frac{1}{2\pi}\right) \tag{21}$$

Therefore, we arrive at the formula for computing the source term $f(\mathbf{x})$:

$$f(\mathbf{x}) = 4\sum_{j=1}^{n_s} b_j \left(G_j(\mathbf{x}) - \frac{1}{2\pi}\right) \tag{22}$$

Similar arguments yield the following expression:

$$f(\mathbf{x}) = \lambda^2 \sum_{j=1}^{n_s} b_j H_j(\mathbf{x}) \tag{23}$$

for Formulation 2 in the two-dimensional case, respectively. Similar expressions can be obtained for higher-dimensional problems.

4. NUMERICAL RESULTS AND DISCUSSION

In this section, we present the numerical results obtained using the general numerical scheme described in Section 3, namely the MFS in conjunction with the TSVD. The effect of regularization, as well as the stability of the scheme with respect to the noise added into the data, are carefully investigated. A sensitivity analysis is also performed with respect to two solution parameters and one problem parameter.

4.1. Examples

The solution domains under consideration are given as follows:

Domain 1 (Unit disk: Smooth domain):

$$\Omega = \{(x_1, x_2) | x_1^2 + x_2^2 < 1\} \tag{24}$$

where (r, θ) are the plane polar co-ordinates.

Domain 2 (Square: Piecewise smooth domain):

$$\widehat{\Omega} = \{(x_1, x_2) | 0 < x_1, x_2 < 6\}, \tag{25}$$

Domain 3 (Complex geometry): The configuration of the complicated domain $\widetilde{\Omega}$ is schematically shown in Figure 1(a). Note that it involves two reentrant corners, which are deliberately designed to verify the robustness, efficiency and effectiveness of the proposed scheme when dealing with problems related to a complicated geometry.

DOI: 10.1002/nme

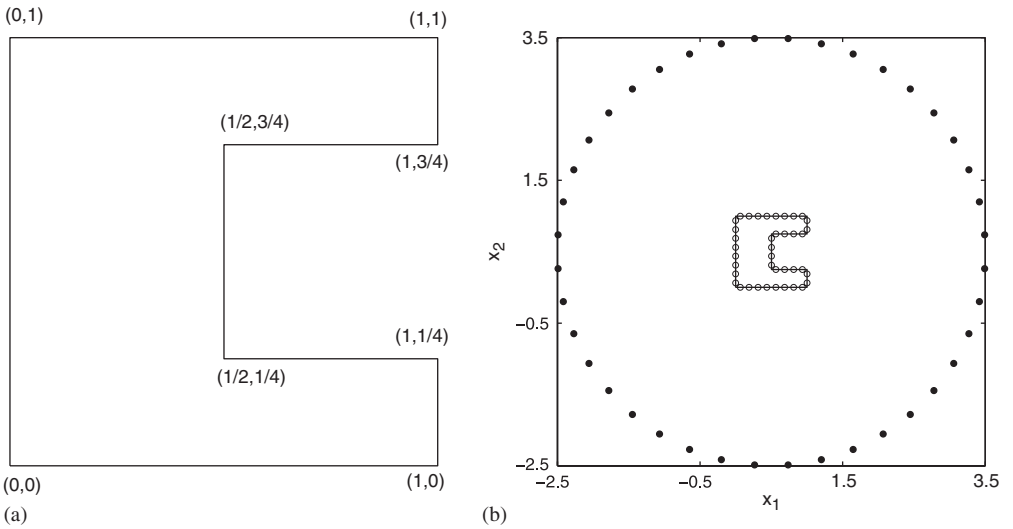

Figure 1. (a) The configuration of the domain with reentrant corners; and (b) the distribution of the source (•) and boundary collocation (○) points.

Table I. Test cases for inverse source problems.

Example	$u(\mathbf{x})$	$f(\mathbf{x})$	Domain
1	$\frac{1}{4}(x_1^2 + x_2^2)$	1	Ω
2	$\frac{1}{4}(x_1^2 + x_2^2)$	1	$\widehat{\Omega}$
3	$-\frac{1}{6}[(x_1 - 6)^3 + (x_2 - 6)^3]$	$12 - x_1 - x_2$	$\widetilde{\Omega}$
4	$e^{x_1}\sin(x_2) + e^{x_1 - x_2}$	$2e^{x_1 - x_2}$	Ω

For the ease of comparison and validation of the numerical results, we consider inverse problems with analytical solutions as listed in Table I. Example 1 is adopted to investigate the effect of the regularization and to perform the sensitivity analysis. Example 2 is a typical benchmark problem considered in References [5–7, 10] and it is investigated for comparison purpose. Example 3 is used to show the efficiency of the proposed numerical scheme for problems with a complicated geometry. Example 4 is analysed to illustrate the application of the combined MFS + TSVD to Formulation 2.

Unless otherwise specified, the fictitious boundary is a circle centred at the origin and of radius 3 for the circular domain Ω, a circle centred at $(3, 3)$ and of radius 10 for the square domain $\widehat{\Omega}$, and a circle centred at $(0.5, 0.5)$ and of radius 3 for the complicated domain $\widetilde{\Omega}$. For all the domains investigated in this study, we consider $n_s = 40$ source points uniformly distributed on the fictitious boundary and $n_b = 40$ collocation points evenly distributed on the accessible part of the boundary Γ_1, which is taken to be the complete boundary Γ. The distribution of the source and boundary collocation points in the case of the complicated domain $\widetilde{\Omega}$ is illustrated in Figure 1(b).

DOI: 10.1002/nme

In real inverse problems, the known boundary data are measured and thus inevitably contaminated by measurement errors. Therefore, the stability of the numerical scheme is of vital importance to obtain physically meaningful results. In our test cases, the simulated noisy data are generated using the following formula:

$$\tilde{b}_i = b_i(1 + \varepsilon\zeta), \quad i = 1, 2, \ldots, 2n_b \tag{26}$$

where ζ is a normally distributed random variable with zero mean and unit standard deviation and ε dictates the level of noise. In our computations, the random variable ζ was realized using the Matlab function `randn()`.

In order to measure the accuracy of the numerical approximation $\tilde{f}$ with respect to the exact solution f, we use the relative error $\mathrm{rerr}(f)$ defined by

$$\mathrm{rerr}(f) = \frac{\sqrt{\sum_{i=1}^{N}(\tilde{f}_i - f_i)^2}}{\sqrt{\sum_{i=1}^{N} f_i^2}} \tag{27}$$

and the maximum error $\mathrm{merr}(f)$

$$\mathrm{merr}(f) = \max_{1 \leqslant i \leqslant N} |\tilde{f}_i - f_i| \tag{28}$$

where $\tilde{f}_i$ and f_i are the numerical and exact solutions evaluated at a point $\mathbf{x}_i$, respectively. Here N is the total number of collocation points in the domain at which both the numerical and exact solutions are evaluated. For all the results presented below, we consider $N = 10{,}000$ for Ω and $\widehat{\Omega}$, and $N = 10{,}800$ for $\widetilde{\Omega}$.

4.2. Effect of regularization

Before presenting the numerical results, it is interesting to investigate how the TSVD improves the accuracy of the numerical results. To do so, we consider Example 1 with 1% noise added into the data. Figure 2(a) shows the error distribution of the numerical solution by the Gauss elimination method. The numerical solution is reasonable in most of the region, as can be seen from Figure 2(a). However, it is highly oscillatory such that the pointwise relative error is as high as 180% at the internal points close to the boundary and hence represents a very inaccurate approximation to the exact heat source $f(\mathbf{x})$. Although not presented, it is reported that similar conclusions have been drawn for the numerical results obtained using the LU factorization and the least-squares method. Thus standard methods could not yield accurate results for noisy data and, consequently, regularization should be employed to retrieve stable numerical solutions in this case.

The numerical results, obtained using the TSVD and the L-curve criterion for determining the optimal regularization parameter, are presented in Figure 2(b). The numerical results indicate that the TSVD, in conjunction with the L-curve criterion, yields very accurate numerical results for noisy data. Therefore, regularization methods are indispensable to guarantee the stability and accuracy of the scheme when the data are contaminated by noise. The regularization method restores the stability of the scheme by filtering out the contributions from the noisy data efficiently and without losing too much information. The numerical results also indicate that the L-curve criterion provides an appropriate regularization parameter for the TSVD.

The main difficulty when using standard methods for solving ill-conditioned systems of linear equations is that the solution is dominated by contributions from very small singular values. From

DOI: 10.1002/nme

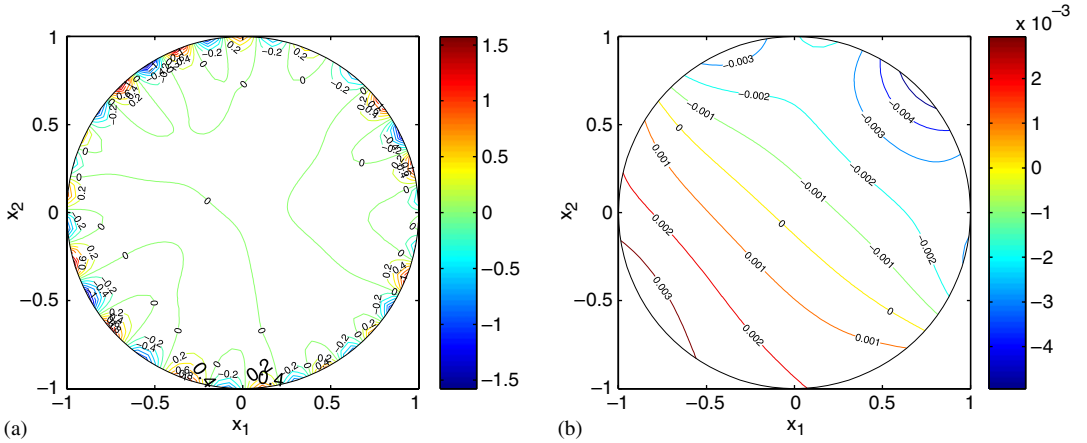

Figure 2. The error distribution for the numerical heat source $f(\mathbf{x})$ obtained using 1% noise added into the data: (a) the Gauss elimination method; and (b) the TSVD, for Example 1.

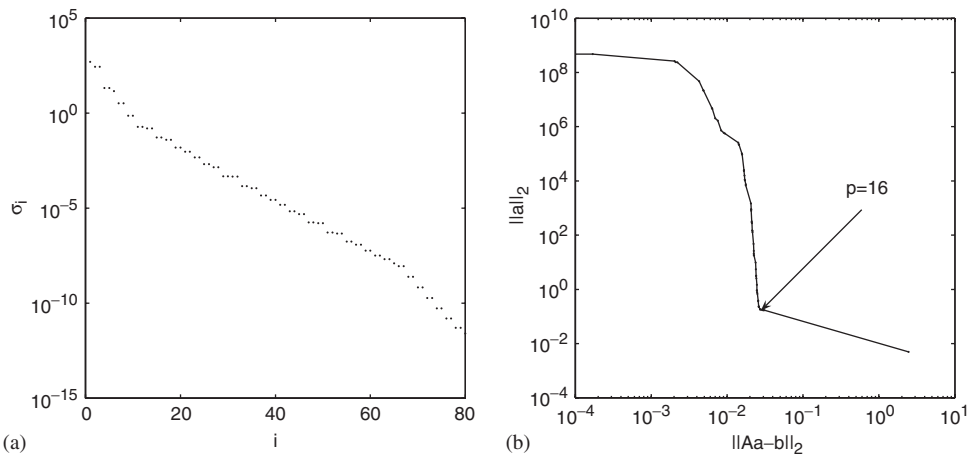

Figure 3. (a) The singular value spectrum; and (b) the L-curve, for Example 1 with 1% noise added into the data.

Figure 3(a) it can be seen that there are numerous small singular values in the singular value spectrum of the matrix $\mathbf{A}$. Furthermore, the singular values decay gradually to zero without any obvious gap and eventual cluster at zero. This is a characteristic for matrices arising from Fredholm integral equations of the first kind [33] to which the MFS is mathematically equivalent. The condition number of the interpolation matrix $\mathbf{A}$ in the case of Example 1 is $\text{Cond}(\mathbf{A}) = 2.02 \times 10^{14}$ and this is enormous in comparison with the small size of the matrix $\mathbf{A}$, namely 80×80.

The L-curve obtained in the case of Example 1 with 1% noise added into the data is shown in Figure 3(b). The L-curve consists of two distinct parts, namely a horizontal part and a vertical one, which, intuitively speaking, correspond to under-regularization and over-regularization, respectively. A good tradeoff between the solution and residual norms is achieved at the corner of

DOI: 10.1002/nme

the L-curve and the optimal regularization parameter is usually chosen such that it corresponds to this corner.

4.3. Sensitivity analysis

In this section, we investigate the sensitivity of the numerical results with respect to two solution parameters, i.e. the number of source points, n_s, and the distance, D, between the fictitious and physical boundaries, and one problem parameter, i.e. the measure of the accessible part of the boundary, meas(Γ_1).

The results for Example 1, obtained using 1% noise added into the data, various numbers of source points and the optimal regularization parameter chosen according to the L-curve criterion, are shown in Figure 4(a). Although not presented here, it is reported that similar results have been obtained for the other examples analysed. It can be seen from Figure 4(a) that the errors rerr(f) and merr(f) decrease until the number of source points reaches the value $n_s = 8$, after which a further increase in the number of source points does not improve substantially the accuracy of the numerical results. The numerical results are practically the same for $n_s \geqslant 8$ in the case of Example 1 and this indicates that accurate numerical results can be obtained using even a relatively small number of source points.

Next, we investigate the sensitivity of the numerical results with respect to the distance $D = R - 1$ between the physical and fictitious boundaries, where R is the radius of the fictitious boundary. The numerical results for Example 1, obtained using 1% noise added into the data and various values for the source radius R are illustrated in Figure 4(b). The accuracy of the numerical results improves before the radius R approaches a specific value, namely $R = 1.5$, after which a further increase of R does not produce any significant improvement in the accuracy achieved. The accuracy of the numerical results is practically the same for $1.5 \leqslant R \leqslant 15$ and, consequently, it is relatively independent of the radius R. Therefore, the TSVD mitigates the critical dependence of the accuracy

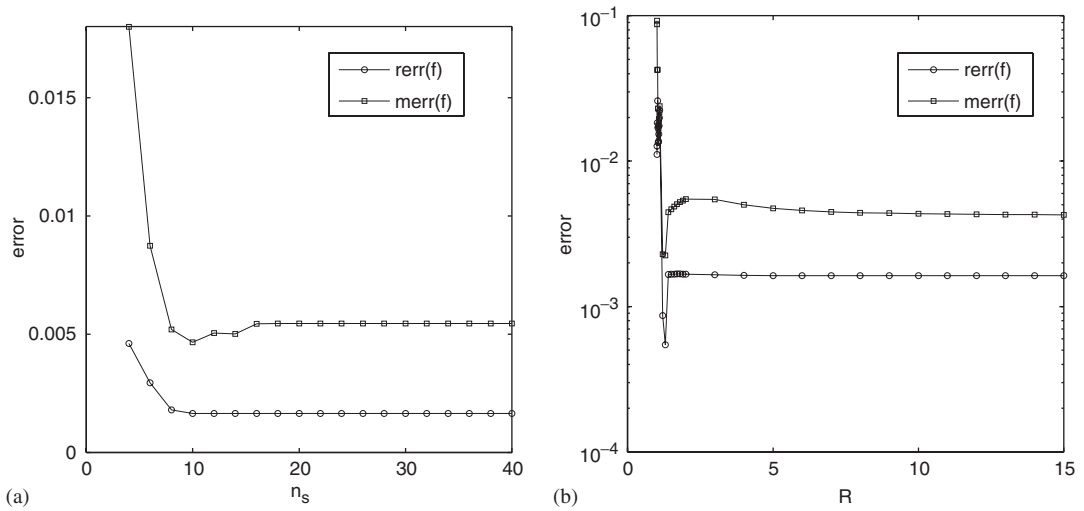

Figure 4. The numerical results obtained using 1% noise added into the data: (a) various numbers of source points n_s; and (b) various values for the source radius R, for Example 1.

DOI: 10.1002/nme

of the numerical results on the location of the source points, as in the case of forward problems subjected to exact and noisy data [41, 42]. It is interesting to note that the numerical results obtained using very large values of the radius R, e.g. $R = 10\,000$, are still in excellent agreement with their corresponding analytical solutions and the accuracy in the numerical solution deteriorates only slightly in comparison with that obtained using $R = 15$. A similar behaviour has been observed for the other examples analysed in this study.

In order to analyse the sensitivity of the proposed method with respect to the measure of the accessible boundary Γ_1, we consider $\Gamma_1 = \{(r, \theta) | r = 1, 0 \leqslant \theta < \alpha\}$, where the polar angle $\alpha \in [\pi/8, 2\pi]$. The accuracy of the numerical results for the heat source in the case of Example 1, obtained using exact and noisy (1%) data, and various values for the parameter α, are illustrated in Figures 5(a) and (b), respectively. The TSVD can improve the accuracy of the numerical results significantly when the data is exact, usually by two orders in magnitude. Figures 6(a) and (b) present the numerical results for Example 1, obtained with exact data, $\alpha = \pi/4$, and using the Gauss elimination method and TSVD, respectively, where the regularization parameter is $p = 38$. The maximum error for the numerical results retrieved when employing the Gauss elimination method is 3.99×10^{-1}, while its corresponding value obtained when using the TSVD is 6.72×10^{-4}. From Figures 5(a) and 6(b) it can be seen that a small part of the accessible boundary Γ_1, i.e. $\alpha = \pi/4$, is sufficient for obtaining accurate numerical results, provided that exact data are available. The numerical results improve significantly as the polar angle α increases, i.e. meas(Γ_1) increases, for both exact and noisy data, as can be noted from Figures 5(a) and (b), respectively. It should be mentioned that, as expected, the numerical results retrieved with noisy data are more inaccurate than those obtained when exact data are available. The error distribution for the numerical heat source $f(\mathbf{x})$ at interior points of the solution domain, for Example 1, obtained using various values of the polar angle α and 1% noise added into the data, are shown in Figures 7(a) and (b), respectively. Here, the truncation number, which is the regularization parameter for the TSVD,

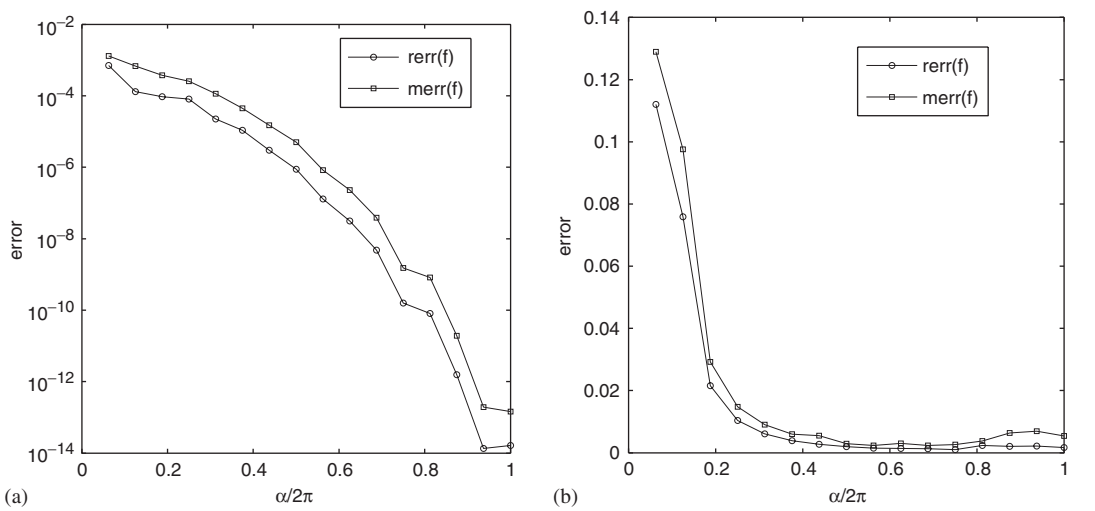

Figure 5. The numerical results obtained using the TSVD, various values of the polar angle α: (a) exact data; and (b) 1% noise added into the data, for Example 1.

DOI: 10.1002/nme

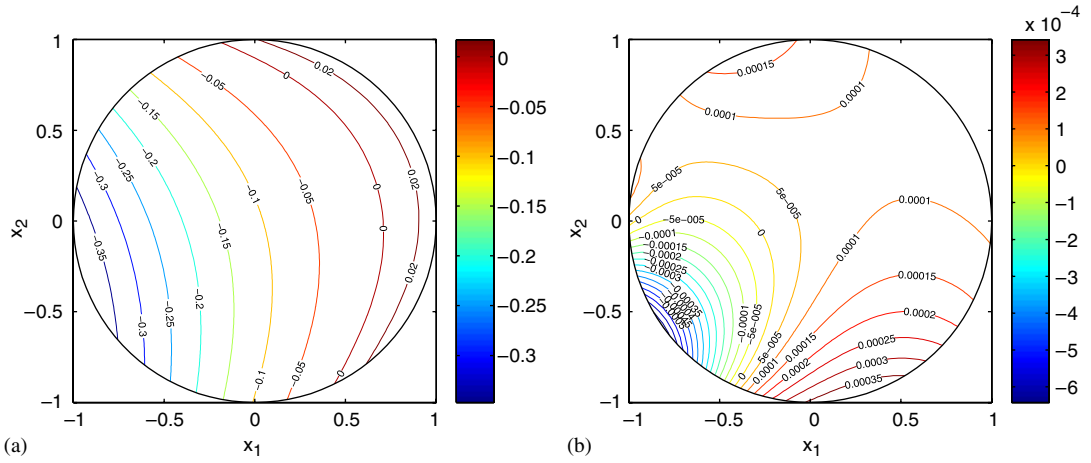

Figure 6. The error distribution for the numerical heat source obtained using exact data, $\alpha = \pi/4$: (a) Gauss elimination method; and (b) the TSVD, for Example 1.

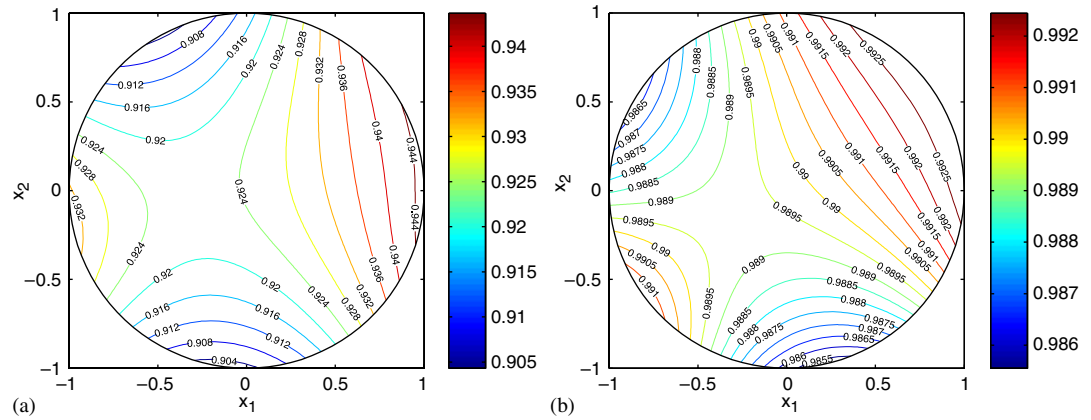

Figure 7. The numerical heat source obtained using 1% noise added into the data: (a) $\alpha = \pi/4$; and (b) $\alpha = \pi/2$, for Example 1.

was found to be $p = 8$. It can be seen from these figures that the numerical results retrieved for $f(\mathbf{x})$ with $\alpha = \pi/4$ represent reasonable approximations for their corresponding exact values, whilst an excellent agreement between the analytical and numerical solutions is achieved for $\alpha \geqslant \pi/2$. From the numerical results presented in Figures 5–7, we can conclude that the proposed scheme is very robust for the inverse source problem. Moreover, a small accessible part of the boundary is sufficient for obtaining accurate numerical results when either exact or noisy data are available.

DOI: 10.1002/nme

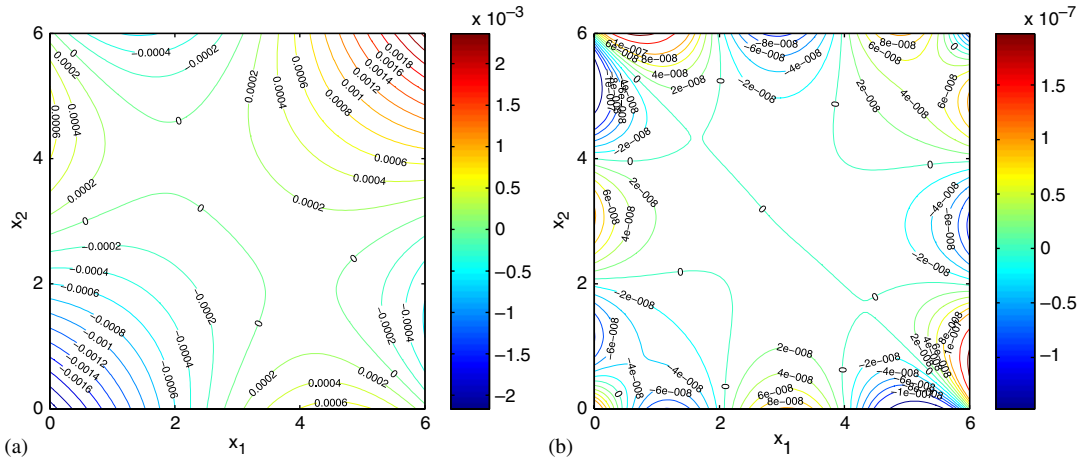

Figure 8. The error distribution for the numerical heat source obtained using exact data and various numbers of source points, namely: (a) $n_s = 8$; and (b) $n_s = 20$, for Example 2.

4.4. *Stability of the method*

The proposed numerical scheme is extremely accurate for problems with exact data. For instance, in the case of Example 2, eight source points provide a very good numerical approximation for the exact heat source, e.g. the maximum error is 2.45×10^{-3}, as presented in Figure 8(a). It should be mentioned that these numerical results are comparable with those reported by Trlep *et al.* [7], who found the maximum error of around 3.37% for the same example. However, the results reported by Trlep *et al.* [7] were obtained using 128 boundary elements and involving an optimization procedure, such as the Fletcher method, and therefore they are computationally much more expensive. The error distribution for the numerical results obtained using 20 source points for Example 2 is illustrated in Figure 8(b), with the maximum error being 2.13×10^{-7}. It should be noted that the present results also seem to be slightly more accurate than those reported by Farcas *et al.* [10].

The striking accuracy of the present numerical results is due to the exponential convergence property of the MFS [12] in the case of smooth solutions. This illustrates clearly the computational efficiency of the proposed numerical scheme since only matrices of very small size are involved in the solution procedure. It is worth mentioning that, although not presented herein, similar conclusions have been drawn for the other examples investigated in this study.

The numerical heat source obtained for Example 1, using various amounts of noise added into the data, are presented in Figures 9(a) and (b). Even for a relatively high amount ($\varepsilon = 2\%$) of noise added into the data, the numerical results retrieved for the heat source represent good approximations for their analytical values. In addition, the numerical heat sources converge towards their corresponding exact solutions as the amount of noise decreases. Hence the MFS, in conjunction with the TSVD, provides stable numerical solutions to the inverse source problem associated with steady-state heat conduction.

The values for the accuracy errors rerr(f) and merr(f), the condition number Cond($\mathbf{A}$) of the interpolation matrix $\mathbf{A}$ and the regularization parameter p, as given by the L-curve criterion, are

DOI: 10.1002/nme

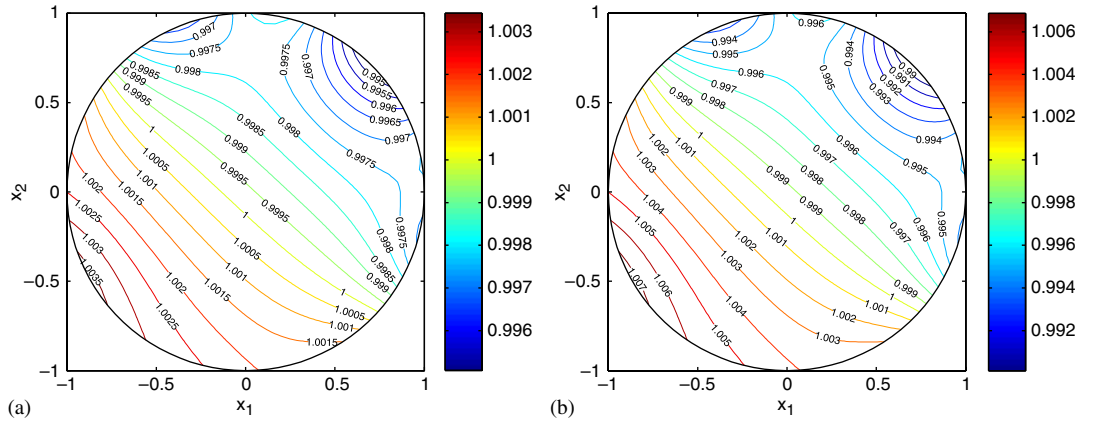

Figure 9. The numerical heat source obtained using various amount of noise added into the data, namely: (a) 1%; and (b) 2%, for Example 1.

Table II. The accuracy of the numerical results for the test cases with 2% noisy data.

Example	Cond(**A**)	p	rerr(f)	merr(f)
1	2.02×10^{14}	16	3.30×10^{-3}	1.09×10^{-2}
2	1.35×10^{15}	18	5.05×10^{-3}	1.58×10^{-2}
3	1.97×10^{19}	12	2.77×10^{-2}	6.22×10^{-1}
4	5.13×10^{13}	24	1.75×10^{-2}	2.50×10^{-1}

presented in Table II, obtained with 2% noise added into the data for all the examples investigated. It is worth mentioning that the accuracy of the numerical results is maintained at a high level, with the error comparable to the amount of noise added into the data.

Similar results have been obtained for Example 2 and these are illustrated in Figure 10. Example 2 has been previously solved by Farcas *et al.* [10] using the DRM-BEM and radial basis functions to approximate the source term. The numerical results presented in our study seem to be more accurate than those obtained by Farcas *et al.* [10] for both exact and noisy data. However, the present scheme avoids singular integration, features fast convergence for smooth solution, is computationally more efficient and enables an easier numerical implementation.

The scheme works equally well for inverse source problems in domains exhibiting a complicated geometry. To illustrate this, the numerical results retrieved for Example 3 using various amounts of noise added into the data are presented in Figure 11. From this figure it can be seen that the numerical solutions for the heat source converge to their corresponding analytical solutions as the amount of noise decreases. The accuracy obtained for the numerical results in the case of Example 3 is comparable with that retrieved for Examples 1 and 2, see e.g. Table II. It should be noted that the analytical solution corresponding to Example 3 is smooth and this is a necessary condition in order to guarantee the exponential convergence of the MFS. In the case of non-smooth solutions, the accuracy of the numerical solutions may be influenced by the geometry of the domain [43], but this is beyond the scope of the present investigation.

DOI: 10.1002/nme

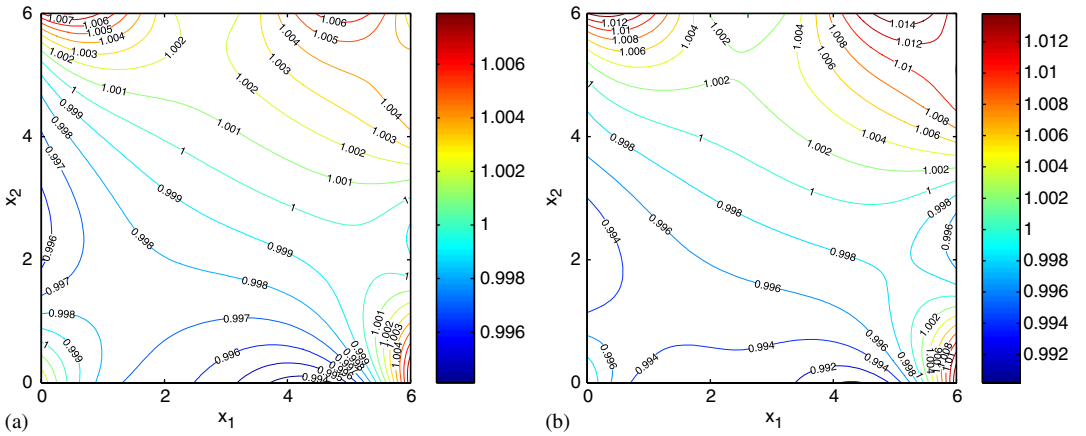

Figure 10. The numerical heat source obtained using various amount of noise added into the data, namely: (a) 1%; and (b) 2%, for Example 2.

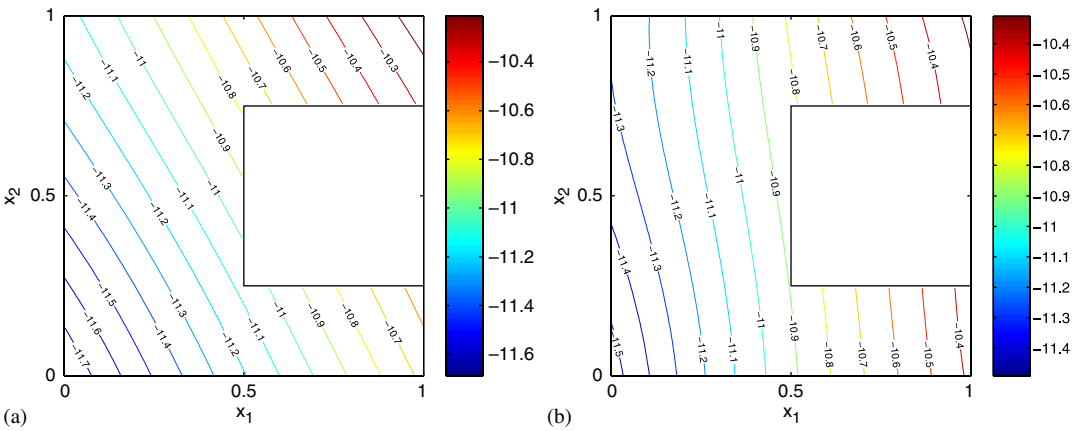

Figure 11. The numerical heat source obtained using various amount of noise added into the data, namely: (a) 1%; and (b) 2%, for Example 3.

So far, the combined MFS + TSVD scheme has been applied to Formulation 1. We now turn to Formulation 2, i.e. Example 4. The numerical results for Example 4, obtained using various amounts of noise added into the data are presented in Figure 12. From this figure it can be seen that better approximations to the analytical solutions are obtained as the amount of noise decreases, i.e. the stability of the proposed scheme is checked for Formulation 2 as well. Furthermore, for the same amount of noisy data on the boundary, the accuracy of the numerical heat source for Example 4 is comparable with that retrieved in the case of Examples 1–3, as depicted from Table II. Therefore, we can conclude that the proposed scheme could easily accommodate other *a priori* assumptions on the heat source.

DOI: 10.1002/nme

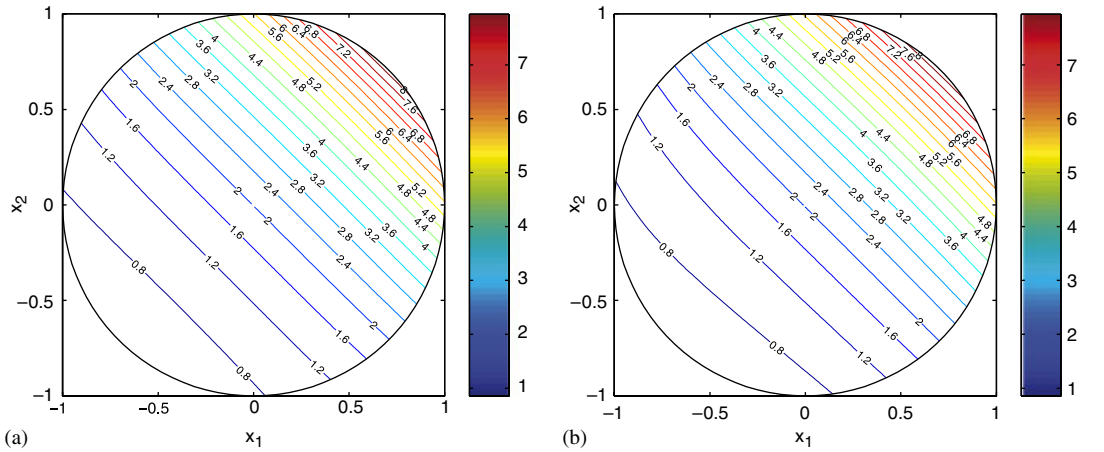

Figure 12. The numerical heat source obtained using various amount of noise added into the data, namely: (a) 1%; and (b) 2%, for Example 4.

Although not presented, it is reported that numerous other numerical experiments have been performed and the same conclusions have been drawn. Overall, it can be concluded that the proposed scheme is computationally efficient, robust, accurate, stable with respect to decreasing the amount of noise added into the data and convergent with respect to increasing the number of source points and the distance between the fictitious and physical boundaries. Furthermore, the approximation of the solution and its derivatives on the entire solution domain are readily available by simple and direct function evaluations.

5. CONCLUSIONS

In this paper, an efficient, accurate, convergent and stable numerical scheme for solving inverse source problems associated with the steady-state heat conduction was proposed. The present numerical procedure was based on the MFS, in conjunction with a popular regularization method, namely the TSVD. The regularization parameter was determined by the L-curve criterion, which assumes no *a priori* knowledge about the noise added into the data. Numerical results for both exact and noisy data have been presented. The numerical results obtained have shown that the proposed scheme is a competitive alternative to existing methods for solving inverse source problems associated with steady-state heat conduction.

There are several potential extensions of the present method. Firstly, the proposed numerical procedure can also be applied to inverse source problems associated with other elliptic partial differential equations, such as the Helmholtz equation [44]. Secondly, the proposed scheme can be easily extended to recover the γ-harmonic source associated with anisotropic heat conduction problems [3]. Thirdly, iterative regularization methods [45], such as conjugate gradient-type methods and the GMRES, may be employed to solve large-scale problems since computing singular value decomposition for large-scale matrices is computationally prohibitive. However, these are deferred to future work.

DOI: 10.1002/nme

ACKNOWLEDGEMENTS

The authors would like to thank Prof. Tuong Ha-Duong for his kind provision of relevant literature and the two anonymous referees for their constructive comments and suggestions.

REFERENCES

1. Isakov V. *Inverse Source Problems*. American Mathematical Society: Providence, Rhode-Island; 1989.
2. El Badia A, Ha Duong T. Some remarks on the problem of source identification from boundary measurements. *Inverse Problems* 1998; **14**(4):883–891.
3. El Badia A. Inverse source problem in an anisotropic medium by boundary measurements. *Inverse Problems* 2005; **21**(5):1487–1506.
4. Ling L, Hon YC, Yamamoto M. Inverse source identification for Poisson equation. *Inverse Problems in Science and Engineering* 2005; **13**(4):433–447.
5. Kagawa Y, Sun Y, Matsumoto O. Inverse solution of Poisson equation using DRM boundary element model—Identification of space charge distribution. *Inverse Problems in Engineering* 1995; **1**(2):247–265.
6. Sun Y, Kagawa Y. Identification of electric charge distribution using dual reciprocity boundary element models. *IEEE Transactions on Magnetics* 1997; **33**(2):1970–1973.
7. Trlep M, Hamler A, Hribernik B. The use of DRM for inverse problems of Poisson's equation. *IEEE Transactions on Magnetics* 2000; **36**(4):1649–1652.
8. Matsumoto T, Tanaka M, Tsukamoto T. Source identification using boundary element method with dual reciprocity method. In *Advances in Boundary Element Techniques IV*, Gallego R, Aliabadi MH (eds). University of London: Queen Mary, 2003; 177–182.
9. Matsumoto T, Tanaka M, Tsukamoto T. Identifications of source distributions using BEM with dual reciprocity method. In *Inverse Problems in Engineering Mechanics IV*, Tanaka M (ed.). Elsevier Science: Amsterdam, New York, 2003; 127–135.
10. Farcas A, Elliott L, Ingham DB, Lesnic D, Mera NS. A dual reciprocity boundary element method for the regularized numerical solution of the inverse source problem associated to the Poisson equation. *Inverse Problems in Engineering* 2003; **11**(2):123–139.
11. El Badia A, Ha Duong T, Moutazaim F. Numerical solution for the identification of source terms from boundary measurements. *Inverse Problems in Engineering* 2000; **8**(4):345–364.
12. Golberg MA, Chen CS. The method of fundamental solution for potential, Helmholtz and diffusion problems. In *Boundary Integral Methods—Numerical and Mathematical Aspects*, Golberg MA (ed.). Computational Mechanics Publications: Southampton, 1998; 103–176.
13. Fairweather G, Karageorghis A. The method of fundamental solutions for elliptic boundary value problems. *Advances in Computational Mathematics* 1998; **9**(1–2):69–95.
14. Cho HA, Golberg MA, Muleshkov AS, Li X. Trefftz methods for time-dependent partial differential equations. *Computers*, *Materials and Continua* 2004; **1**(1):1–37.
15. Marin L, Lesnic D. The method of fundamental solutions for the Cauchy problem associated with two-dimensional Helmholtz-type equations. *Computers and Structures* 2005; **83**(4–5):267–278.
16. Marin L. A meshless method for the numerical solution of the Cauchy problem associated with three-dimensional Helmholtz-type equations. *Applied Mathematics and Computation* 2005; **165**(2):355–374.
17. Jin B, Zheng Y. A meshless method for some inverse problems associated with the Helmholtz equation. *Computer Methods in Applied Mechanics and Engineering* 2006; **195**(19–22):2270–2288.
18. Jin B, Zheng Y. Marin L. The method of fundamental solutions for some inverse boundary value problems associated with steady-state anisotropic heat conduction. *International Journal for Numerical Methods in Engineering* 2006; **65**(11):1865–1891.
19. Marin L, Lesnic D. The method of fundamental solutions for the Cauchy problem in two-dimensional linear elasticity. *International Journal of Solids and Structures* 2004; **41**(13):3425–3438.
20. Marin L. A meshless method for solving the Cauchy problem in three-dimensional elastostatics. *Computers and Mathematics with Applications* 2005; **50**(1–2):73–92.
21. Hon YC, Wei T. A fundamental solution method for inverse heat conduction problem. *Engineering Analysis with Boundary Elements* 2004; **28**(5):489–495.
22. Hon YC, Wei T. The method of fundamental solutions for solving multidimensional inverse heat conduction problems. *CMES—Computer Modeling in Engineering and Science* 2005; **7**(2):119–132.

DOI: 10.1002/nme

23. El Badia A, Ha-Duong T. An inverse source problem in potential analysis. *Inverse Problems* 2000; **16**(3):651–663.
24. Sober E. The principle of parsimony. *British Journal of Philosophy Science* 1981; **32**(2):145–156.
25. Wood AS, Tupholme GE, Bhatti MIH, Heggs PJ. Steady-state heat transfer through extended plane surfaces. *International Communications in Heat and Mass Transfer* 1995; **22**(1):99–109.
26. Kupradze VD, Aleksidze MA. The method of functional equations for the approximate solution of certain boundary value problems. *USSR Computational Mathematics and Mathematical Physics* 1964; **4**(1):82–126.
27. Mathon R, Johnston RL. The approximate solution of elliptic boundary-value problems by fundamental solutions. *SIAM Journal on Numerical Analysis* 1977; **14**(4):638–650.
28. Fairweather G, Karageorghis A, Martin PA. The method of fundamental solutions for scattering and radiation problems. *Engineering Analysis with Boundary Elements* 2003; **27**(7):759–769.
29. Kythe PK. *Fundamental Solutions for Differential Operators and Applications*. Birkhäuser: Boston, 1996.
30. Cheng AH-D, Antes H, Ortner N. Fundamental solutions of products of Helmholtz and polyharmonic operators. *Engineering Analysis with Boundary Elements* 1994; **14**(2):187–191.
31. Poullikkas A, Karageorghis A, Georgiou G. Method of fundamental solutions for harmonic and biharmonic boundary value problems. *Computational Mechanics* 1998; **21**(4–5):416–423.
32. Mitic P, Rashed YF. Convergence and stability of the method of meshless fundamental solutions using an array of randomly distributed source. *Engineering Analysis with Boundary Elements* 2004; **28**(2):143–153.
33. Hansen PC. *Rank-deficient and Discrete Ill-posed Problems*: *Numerical Aspects of Linear Inversion*. SIAM: Philadelphia, 1998.
34. Hansen PC, O'Leary DP. The use of the L-curve in the regularization of discrete ill-posed problems. *SIAM Journal on Scientific Computing* 1993; **14**(6):1487–1503.
35. Chen LY, Chen JT, Hong HK, Chen CH. Application of Cesàro mean and the L-curve for the deconvolution problem. *Soil Dynamics and Earthquake Engineering* 1995; **14**(5):361–373.
36. Hanke M. Limitations of the L-curve method in ill-posed problems. *BIT Numerical Mathematics* 1996; **36**(2): 287–301.
37. Vogel CR. Non-convergence of the L-curve regularization parameter selection method. *Inverse Problems* 1996; **12**(4):535–547.
38. Guerra V, Hernandez V. Numerical aspects in locating the corner of the L-curve. In *Approximation*, *Optimization and Mathematical Economics*, Lassonde M (ed.). Springer-Verlag: Heidelberg, 2001; 121–131.
39. Kaufman L, Neumaier A. PET regularization by envelope guided conjugate gradients. *IEEE Transactions on Medical Imaging* 1996; **15**(3):385–389.
40. Castellanos JL, Gomez S, Guerra V. The triangle method for finding the corner of the L-curve. *Applied Numerical Mathematics* 2002; **43**(4):359–373.
41. Ramachandran PA. Method of fundamental solutions: singular value decomposition analysis. *Communications in Numerical Methods in Engineering* 2002; **18**(11):789–801.
42. Jin B. A meshless method for the Laplace and biharmonic equations subjected to noisy boundary data. *CMES—Computer Modeling in Engineering and Science* 2004; **6**(3):253–261.
43. Karageorghis A. Modified methods of fundamental solutions for harmonic and biharmonic problems with boundary singularities. *Numerical Methods for Partial Differential Equations* 1992; **8**(1):1–19.
44. Marengo EA, Devaney AJ, Ziolkowski RW. Inverse source problem and minimum energy sources. *Journal of Optical Society of America* 2000; **17**(1):34–45.
45. Hanke M, Hansen PC. Regularization methods for large-scale problems. *Surveys on Mathematics for Industry* 1993; **3**(4):253–315.

DOI: 10.1002/nme